International Journal of Modern Physics B
Vol. 26, No. 3 (2012) 1250017 (18 pages)

DOI: 10.1142/S0217979212500178

World Scientific
www.worldscientific.com

EVOLUTION OF INTERFERENCE PATTERNS OF SUPERFLUID FERMI GASES RELEASED FROM A TWO-DIMENSIONAL OPTICAL LATTICE

SUJUAN LIU

State Key Laboratory of Precision Spectroscopy and Department of Physics, East China Normal University, Shanghai 200062, China
liusuj122000@163.com

WEN WEN

Department of Mathematics and Physics, Hohai University, Changzhou Campus, 200 Jingling Road North, Changzhou, Jiangsu 213002, China
Wenw@hhuc.edu.cn

GUOXIANG HUANG*

State Key Laboratory of Precision Spectroscopy and Department of Physics, East China Normal University, Shanghai 200062, China
gxhuang@phy.ecnu.edu.cn

Received 27 June 2011

We study interference patterns and their time evolution of a superfluid fermionic gas released from a two-dimensional (2D) optical lattice below and above Feshbach resonance. We calculate initial distribution of many subcondensates formed in a combined potential of a parabolic trap and a 2D optical lattice in the crossover from Bardeen–Cooper–Schrieffer (BCS) superfluid to a Bose–Einstein condensate (BEC). By using Feynman propagator method combined with numerical simulations we investigate the interference patterns of the subcondensates for two different cases. One is when both the parabolic trap and optical lattice are switched off. In this case, interference pattern displays a main peak and many secondary peaks. The distance between these interference peaks grows as time increases. The other one is when only the 2D optical lattice is switched off. The interference pattern in this case is found to display decay and revival, and such behavior repeats periodically with increasing time. In different regimes of the BCS-BEC crossover, coherent arrays of interference patterns show different features, which can be used to characterize experimentally different properties in different superfluid regimes of the BCS–BEC crossover.

Keywords: Bose–Einstein condensation; superfluid fermionic atomic gases; BCS–BEC crossover; order-parameter; coherent property.

*Corresponding author.

1. Introduction

In recent years, study of superfluid Fermi gases has opened a new frontier of research in the physics of ultracold matters. One of important topics in this field is the property of neutral fermionic atoms in the crossover from Bardeen–Cooper–Schrieffer (BCS) superfluid to a Bose–Einstein condensate (BEC). The understanding of BCS–BEC crossover not only has fundamental theoretical interest in condensed-matter physics, but also has important applications for high-temperature superconductivity and other significant physical problems. Thanks to the successful application of magnetic-field induced Feshbach resonance, different superfluid regimes can be realized and manipulated in a controllable way, leading to explosive growth of research activity on the BCS–BEC crossover in ultracold fermionic atomic gases.[1–4]

Optical lattices, i.e., regular arrays of many small potential wells created by one or more sets of orthogonal intersecting laser beams, provide a periodic potential for the motion of ultracold atomic gases. Fermionic atoms in optical lattices can be used to simulate the motion of electrons in metals and semiconductors. Such quantum simulation has many advantages comparing with using other systems.[5] First, the period of an optical lattice potential is macroscopically large, and hence advantageous for simplifying experimental measurements greatly. Second, the optical lattice can be switched off, which is impossible in metals and semiconductors, and both the period and intensity of the periodic potential formed by laser beams can be manipulated and adjust at will. Third, it is easy to create one-dimensional (1D), two-dimensional (2D) and three-dimensional (3D) optical lattices which are static and free of defects,[5] or artificially design quasi-periodic and disordered potentials in a controllable way.[6] As did in superfluid bosonic atoms, there are a lot of research on superfluid fermionic atomic gases in optical lattices.[1–4,7–9]

Coherent property is an important topic in the study of superfluid fermionic atomic gases. The most effective method for the observation of coherent property is the measurement of interference patterns of superfluid Fermi gases when released from optical lattices. In the remarkable experiment carried out by MIT group,[10] high-contrast interference patterns of an ultracold fermionic atom (^{6}Li) gas have been observed, which has been recognized as the most direct and powerful experimental evidence of good coherency of superfluid Fermi gases in the BCS–BEC crossover.

However, above mentioned experimental and theoretical works on interference patterns of superfluid Fermi gases are only for the case of 3D optical lattices. It is natural to ask the question how about the situation if a superfluid Fermi gas is released from a 2D optical lattice and what new characters will appear. It is just this topic that will be addressed here. To the best of our knowledge, up to now there is no study on interference patterns and their time evolution of superfluid Fermi gases released from 2D optical lattices. In the present work, we consider this problem theoretically and show that, in different regimes of the BCS–BEC

crossover, coherent arrays of interference patterns and their evolution show quite different features in comparison with the case of 3D optical lattices, which can be used to characterize experimentally different properties in different superfluid regimes of the BCS–BEC crossover.

The paper is arranged as follows. In Sec. 2, we give a simple introduction of an order-parameter equation used to describe the dynamics of fermionic-pair condensate. In Sec. 3, by solving the order-parameter equation we calculate the initial distribution of fermionic-pair subcondensates formed in a 2D optical lattice and a parabolic potential trap. Coherent evolution of the subcondensates are investigated in two different cases, including the one when both the optical lattice and the parabolic trap are switched off, and the other one when only the 2D optical lattice is switched off. Interference patterns of both cases are calculated by means of Feynman propagator combined with numerical simulations. Section 4 contains a discussion on the limitation of applicability of the order-parameter equation and summary of our main results of the present work.

2. Time Evolution of Interference Patterns

2.1. *Initial distribution of subcondensates confined in parabolic trap and optical lattice*

We consider a superfluid Fermi gas that has an equal number of fermionic atoms (i.e., ^{6}Li or ^{40}K) occupying two different internal (spin) states. At zero temperature, all atoms are paired and condensed atomic pair density is $n_s = n/2$, where n is atomic density. The transition from BCS superfluid to BEC can be realized by means of magnetic-field induced Feshbach resonance, and hence manipulating s-wave scattering length a_s.[1–3] When $a_s < 0$ ($a_s > 0$), the system is prepared in BCS (BEC) regime. Defining a dimensionless interaction parameter $\eta \equiv 1/(k_F a_s)$, where $k_F = (3\pi^2 n)^{1/3}$ is Fermi wavenumber, one can distinguish several different superfluid regimes, i.e., BCS regime ($\eta < -1$), BEC regime ($\eta > 1$), and BEC-BCS crossover regime ($-1 < \eta < 1$). The case $\eta = -\infty$ ($\eta = +\infty$) is called BCS (BEC) limit and the case $\eta = 0$ is called unitarity limit. Up to now both theoretical and experimental studies verify that the transition from BCS regime to BEC regime is smooth,[1–3] and hence the study on physical properties of the superfluid Fermi gas in various superfluid regimes can be done in a unified way.

In principle, the coherent property of the superfluid Fermi gas in the BCS–BEC crossover can be studied based on a microscopic theory. In this approach one starts from a model many-body Hamiltonian that includes main characters of ultracold fermionic atomic gases. However, because the fermionic atom pairs in present system are confined in a combined potential of an optical trap and an optical lattice, the inhomogeneous and mesoscopic features of the system makes the microscopic approach difficult. As a first step, one can resort to a phenomenological approach which can simplify the problem considerably. Notice that for shallow optical lattice depth the system is within superfluid regime, and hence at ultralow temperature the

condensed fermionic atom pairs do not decay into single atoms due to the existence of energy gap in excitation spectrum. The dynamics of such perfect superfluid can be well described phenomenologically by using an order-parameter equation.[11–25] Different superfluid regimes can be characterized by an equation of state, which can be obtained by quantum Monte-Carlo simulation or by other methods.[26–28] The order-parameter equation captures dominant feature that the superfluid exhibits macroscopically. Recently, the method of order-parameter equation has been used to investigate linear collective excitations, ballistic expansion, and solitons in superfluid Fermi gases, and the results obtained agree quite well with experimental ones.[11–25]

The order-parameter equation valid for zero temperature takes the form

$$i\hbar\frac{\partial\Psi_s}{\partial t} = \left[-\frac{\hbar^2\nabla^2}{2M} + V_s^{\rm ho}(\mathbf{r}) + \mu_s(n_s)\right]\Psi_s\,. \tag{1}$$

where $\mathbf{r} \equiv (x, y, z)$, $\Psi_s(\mathbf{r}, t)$ is the order-parameter (or called condensate wavefunction), $M = 2m$ is the mass of fermionic atomic pair (with m being atomic mass), $V_s^{\rm ho}(\mathbf{r})$ is parabolic trap, which has can be modeled by the linear harmonic oscillator potential[1–3]

$$V_s^{\rm ho}(\mathbf{r}) = \frac{M}{2}[\omega_\perp^2(x^2 + y^2) + \omega_z^2 z^2]\,. \tag{2}$$

with $\omega_\perp$ and ω_z the trapping frequency in transverse (i.e., x and y) and axial (i.e., z) directions, respectively.

The equation of state (also called bulk chemical potential) in Eq. (1) is obtained by local density approximation[a] (LDA) and has the form $\mu_s(n_s) = 2\mu(2n_s)$. Here $\mu(n) = \partial[n\varepsilon(n)]/\partial n$, with $\varepsilon(n)$ being the bulk energy per particle for $V_s^{\rm ho} = 0$ (see Footnote b). By defining $\varepsilon(n) = (3/5)\varepsilon_F\sigma(\eta)$ ($\varepsilon_F = \hbar^2 k_F^2/(2m)$ is Fermi energy), one obtains[13–20]

$$\mu(n) = \varepsilon_F\left[\sigma(\eta) - \frac{\eta}{5}\frac{\partial\sigma(\eta)}{\partial\eta}\right]. \tag{3}$$

Generally, the expression of $\mu(n)$ is very complicated, and hence an analytical result on the dynamics of the system is hard to obtain. A simple treatment is to make a polytropic approximation, which assumes[11–20,30–32] $\mu(n) = \mu^0(n/n^0)^\gamma$, where μ^0 and n^0 are reference chemical potential and particle number density of the system. In the following calculation we take n^0 to be the equilibrium superfluid density at the center of the parabolic potential. Thus one has $\mu^0 = \varepsilon_F[\sigma(\eta^0) - \eta^0\sigma'(\eta^0)/5]$, with $\eta^0 = 1/(k_F^0 a_s)$ and $k_F^0 = (3\pi n^0)^{1/3}$. It is easy to check that in the deep BEC regime (i.e., $\gamma = 1$) Eq. (1) coincides exactly with the one derived by Pieri and Strinati[29] based on Bogoliubov–de Gennes equations for superfluid fermionic pairs.

We assume that the superfluid Fermi gas is prepared in the anisotropic 3D harmonic potential (2). The trapping frequency in the axial direction is much larger

[a]LDA is valid for slowly-varying external potential. The present system fulfills LDA condition.
[b]An interpolating analytical formula for has been given in Ref. 13 for ^{7}Li.

than that in the transverse directions, i.e., $\omega_z \gg \omega_\perp$. Obviously, in equilibrium the system is a large disk-shaped condensate. Then a 2D optical lattice potential of the form

$$V_s^{\rm op}(x,y) = sE_R[\sin^2(qx) + \sin^2(qy)]\,, \tag{4}$$

is added to the system, which forms by two orthogonal intersecting laser beams with wave vector $q = 2\pi/\lambda$ fixed by the wavelength λ of the laser beams. The lattice potential depth is sE_R with recoil energy defined by $E_R = \hbar^2 q^2/(2M)$, where s is a dimensionless parameter controlling the intensity of the laser field. It is expected that the large disk-shaped condensate will become many subcondensates when the 2D optical lattice is switched on. Our aim is to obtain interference patterns of the superfluid Fermi gas. Thus the initial distribution of these subcondensates, described by $\Psi_s(\mathbf{r}, 0)$, must be calculated firstly.

In fact, $\Psi_s(\mathbf{r}, 0)$ we are looking for is nothing but the ground-state solution of the order-parameter equation (1), which is however hard to obtained analytically because Eq. (1) is not only nonlinear but also has variable coefficients. Of course, one can directly integrate Eq. (1) numerically, but such result is not transparent for the physical analysis of interference patterns and their evolution. Here we employ the technique developed in Refs. 33 and 34 to obtain the approximate analytical expression of $\Psi_s(\mathbf{r}, 0)$ when both the parabolic trap and the 2D optical lattice are present.

Notice that the size of the system is much larger than that of each subcondensate. If the optical lattice depth is moderately large the optical lattice potential can be expressed by a superposition of many approximate harmonic potentials, i.e., $V_s^{\rm op} = (M\omega_{\rm op}^2/2)[\sum_{k_x}(x - k_x d)^2 + \sum_{k_y}(y - k_y d)^2]$. Here the effective frequency is defined by $\omega_{\rm op} = 2\sqrt{s}E_R/\hbar$, typically much larger than the frequency of the parabolic potential. Obviously, the presence of 2D optical lattice makes the large, disk-shaped condensate formed in the parabolic trap split into a 2D arrays of weakly coupled, small cigar-shaped subcondensates that are located in minima of the combined potential $V_s = V_s^{\rm ho} + V_s^{\rm op}$.

We assume that typical width of subcondensates is much less than the period $d = \lambda/2$ of the optical lattice and the subcondensates in different lattice sites are fully coherent. In this case the chemical potential of these subcondensates is identical and hence the condensate wavefunction of the system can be obtained by the tight-binding approximation

$$\Psi_s(\mathbf{r}, t) = \sum_{k_x,k_y} \psi_{k_x,k_y}(x, y, z) \exp(-i\mu_G t/\hbar)\,, \tag{5}$$

where μ_G is the chemical potential of the system, k_x and k_y are the central positions of various subcondensates. Substituting Eq. (5) into Eq. (1) we get

$$\left\{ -\frac{\hbar^2\nabla^2}{2M} + \frac{1}{2}M[\omega_\perp^2(x^2 + y^2) + \omega_z^2 z^2] + \frac{1}{2}M\omega_{\rm op}^2[(x - k_x d)^2 \right.$$

$$+(y-k_yd)^2]+\mu_s^0\left(\frac{n_s}{n_s^0}\right)^\gamma\Bigg\}\psi_{k_x,k_y}=\mu_G\psi_{k_x,k_y}\,, \tag{6}$$

where $\mu_s^0=\mu_s(n_s^0)$. In obtaining Eq. (6) the small overlap between adjacent subcondensates is ignored. Using the transformation $x-k_xd\to x$, $y-k_yd\to y$, Eq. (6) becomes

$$\left[-\frac{\hbar^2\nabla^2}{2M}+\frac{1}{2}M\omega_\perp^2[(x+k_xd)^2+(y+k_yd)^2]+\frac{1}{2}M\omega_z^2z^2\right.$$
$$\left.+\frac{1}{2}M\omega_{\rm op}^2(x^2+y^2)+\mu_s^0\left(\frac{n_s}{n_s^0}\right)^\gamma\right]\psi_{k_x,k_y}=\mu_G\psi_{k_x,k_y}\,, \tag{7}$$

which is the equation determining ψ_{k_x,k_y} at the lattice site (k_x,k_y). Because $\omega_{\rm op}\gg\omega_\perp$, it is obvious that, for the subcondensate confined in the lattice site ψ_{k_x,k_y}, one has $x\ll k_xd$ and $y\ll k_yd$, and hence Eq. (7) can be simplified into

$$\left[-\frac{\hbar^2\nabla^2}{2M}+\frac{1}{2}M\omega_z^2z^2+\frac{1}{2}M\omega_{\rm op}^2(x^2+y^2)+\mu_s^0\left(\frac{n_s}{n_s^0}\right)^\gamma\right]\psi_{k_x,k_y}=\mu_{k_x,k_y}\psi_{k_x,k_y}\,, \tag{8}$$

where $\mu_{k_x,k_y}=\mu_G-(M/2)\omega_\perp^2d^2(k_x^2+k_y^2)$, which is the effective chemical potential for the subcondensate at lattice site (k_x,k_y).

By our assumption, we have $\hbar\omega_z\ll\mu_G\ll\hbar\omega_{\rm op}$, and hence all subcondensates in the optical lattice are cigar-shaped with their long axes along z-direction. It is reasonable to assume that the motion of the subcondensates in the x- and y-directions is essentially frozen and hence the wavefunction has the Gaussian form $\phi(x,y)=(\pi a_{\rm op}^2)^{-1/2}\exp[-(x^2+y^2)/(2a_{\rm op}^2)]$ with $a_{\rm op}=\sqrt{\hbar/(M\omega_{\rm op})}$. Taking $\psi_{k_x,k_y}(\mathbf{r})=\phi(x,y)\varphi_{k_x,k_y}(z)$, the 3D Eq. (8) is reduced to a 1D one:

$$\left[-\frac{\hbar^2}{2M}\frac{\partial^2}{\partial z^2}+\frac{1}{2}M\omega_z^2z^2+g_{1D}|\varphi_{k_x,k_y}(z)|^{2\gamma}\right]\varphi_{k_x,k_y}(z)$$
$$=(\mu_{k_x,k_y}-\hbar\omega_{\rm op})\varphi_{k_x,k_y}(z)\,, \tag{9}$$

which describes the cigar-shaped condensate at the lattice site (k_x,k_y). The solution of this equation can be obtained by using Thomas–Fermi approximation,,[1–3] i.e., the kinetic energy term can be disregarded. Thus we obtain

$$\varphi_{k_x,k_y}(z)=\left[\frac{\mu_{k_x,k_y}-\hbar\omega_{\rm op}-\frac{1}{2}M\omega_z^2z^2}{g_{1D}}\right]^{\frac{1}{2\gamma}} \tag{10}$$

with $g_{1D}=\mu_s^0/[(n_s^0\pi a_{\rm op}^2)^\gamma(\gamma+1)]$. Using these results it is readily to get the number of condensed fermionic pairs in the subcondensate located at the lattice site (k_x,k_y)

$$N_{k_x,k_y}=N_{0,0}\left[1-\frac{k_x^2+k_y^2}{k_M^2}\right]^{\frac{1}{\gamma}+\frac{1}{2}}\,, \tag{11}$$

where $k_M^2 = 2(\mu_G - \hbar\omega_{\rm op})/(M\omega_\perp^2 d^2)$. The condition $k_x^2 + k_y^2 \leq k_M^2$ gives the total number of subcondensates, i.e., πk_M^2. In Eq. (11), $N_{0,0}$ is the number of condensed fermionic pairs at the central lattice site, which is given by

$$N_{0,0} = \frac{\pi^{1/2}\Gamma(1/\gamma+1)k_M d}{\Gamma(1/\gamma+3/2)}\left(\frac{M\omega_\perp^2 k_M^2 d^2}{2g_{1D}}\right)^{1/\gamma}\frac{\omega_\perp}{\omega_z}\,. \tag{12}$$

The normalization condition $N = \sum_{k_x,k_y} N_{k_x,k_y}$, here N is the total number of the condensed fermionic pairs in the system, yields

$$k_M = \left[N\frac{\Gamma(1/\gamma+2/3)}{\Gamma(1/\gamma+1)}\frac{(3\gamma+2)}{2\pi^{3/2}\gamma d}\left(\frac{2g_{1D}}{M\omega_\perp^2 d^2}\right)^{1/\gamma}\frac{\omega_z}{\omega_\perp}\right]^{\frac{\gamma}{3\gamma+2}}. \tag{13}$$

Based on the above results we finally obtain the normalized condensate wavefunction of the system in the combined potential of the parabolic trap and the optical lattice at time $t = 0$ (see footnote c)

$$\Psi_s(\mathbf{r}, t=0) = A_n {\sum_{k_x,k_y}}' \left(1 - \frac{k_x^2+k_y^2}{k_M^2}\right)^{\frac{1}{2\gamma}+\frac{1}{4}} \times \exp\left[-\frac{(x-k_x d)^2 + (y-k_y d)^2}{2a_{\rm op}^2}\right]\varphi_{k_x,k_y}(z)\,, \tag{14}$$

where $A_n = [(3\gamma+2)/(2\gamma\pi^2 k_M^2 a_{\rm op}^2)]^{1/2}$ is a normalization constant, the prime in the sum means that the summation for k_x and k_y is taken in the region $k_x^2 + k_y^2 \leq k_M^2$, and $\varphi_{k_x,k_y}(z)$ is a normalized function in z-direction, given by Eq. (10).

In x–y coordinate space, the density distribution of the subcondensates at $t = 0$ is

$$n_s(x, y, t=0) \equiv N\int dz n_s(x, y, z, t=0) = N|\Psi_s(x, y, t=0)|^2\,, \tag{15}$$

where

$$\Psi_s(x, y, t=0) \equiv A_n {\sum_{k_x,k_y}}' \left(1 - \frac{k_x^2+k_y^2}{k_M^2}\right)^{\frac{1}{2\gamma}+\frac{1}{4}} \exp\left[-\frac{(x-k_x d)^2 + (y-k_y d)^2}{2a_{\rm op}^2}\right]. \tag{16}$$

2.2. *Interference patterns and their evolution after switching off both the parabolic trap and optical lattice*

The time evolution of the superfluid Fermi gas after release of the parabolic trap and optical lattice potentials can be obtained through solving the Ginzburg–Gross–Pitaevskii (GGP) equation (1) by taking Eq. (16) as an initial condition. Noticing

[c]In the following, $t = 0$ will be taken as the initial time for free expansion of the superfluid Fermi gas.

that the gas is freely expanded, the interaction among atoms during the expansion is small and thus can be neglected. Thus we can employ famous Feynman propagator method[35] to obtain the condensate wavefunction for any time $t > 0$. It is easy to get

$$\Psi_s(x,y,t) = \int_{-\infty}^{\infty} dx' \int_{-\infty}^{\infty} dy' G(x,y,t;x',y',t'=0)\Psi_s(x',y',t'=0)\,, \tag{17}$$

where the propagator $G(x,y,t;x',y',t'=0)$ is given by

$$G(x,y,t;x',y',t'=0) = \left(\frac{2\pi i\hbar t}{M}\right)^{-1} \exp\left[\frac{iM((x-x')^2+(y-y')^2)}{2\hbar t}\right]. \tag{18}$$

The integration on the right-hand side of Eq. (17) can be done exactly, yielding

$$\Psi_s(x,y,t) = A_n\left(\frac{1}{1+i\alpha}\right) {\sum_{k_x,k_y}}' \left(1-\frac{k_x^2+k_y^2}{k_M^2}\right)^{\frac{1}{2\gamma}+\frac{1}{4}} \times \exp\left[-\frac{(x-k_x d)^2+(y-k_y d)^2}{2a_{\rm op}^2(1+i\alpha)}\right] \tag{19}$$

with a dimensionless parameter $\alpha = \hbar t/Ma_{\rm op}^2$.

Now we discuss the interference patterns and their property in the BCS–BEC crossover. Assume the parabolic potential is highly anisotropic, with trapping frequencies $\omega_\perp = 2\pi\times 200$ Hz and $\omega_z = 2\pi\times 20{,}000$ Hz. The total number of fermionic atomic pairs is $N = 5\times 10^4$ and the laser beam wavelength of the optical lattice is $\lambda = 1064$ nm and laser beam intensity is $s = 5$. Two semi-axes in the radial directions of the laser beam are $R_j^2 = 2\mu_s(0)/(M\omega_j^2)$ $(j = x, y)$. The Fermi energy of the trapped fermions, defined by $E_F = \hbar(6N\omega_x\omega_y\omega_z)^{1/3}$, determines the value $1/k_F^0 = 0.33$ μm. When the dimensionless interaction parameter η^0 takes vales from 4.0, 0.5 to 0, and then to -0.48 and -1.0, we obtain values of η^0, γ, μ_s^0/ε_F^0, and $R_\perp$ $(R_\perp \equiv (R_xR_y)^{1/2})$, given in Table 1.

Shown in Fig. 1 are interference patterns of pair density distribution in the regime BCS–BEC crossover based on the result given by Eq. (19). Parameters are chosen as $(\eta^0, \gamma, \mu_s^0/\varepsilon_F^0) = (0.5, 0.992, 0.358)$, which corresponds to the case (b) of Table 1. The sequent panels in the figure are the interference patterns for time $t = 0$, $t = 0.3\pi/\omega_\perp$, $t = 0.5\pi/\omega_\perp$, $t = 0.7\pi/\omega_\perp$, and $1.0\pi/\omega_\perp$, respectively. We

Table 1. Parameters of the superfluid Fermi gas in the BCS–BEC crossover used in numerical simulations.

	(a)	(b)	(c)	(d)	(e)
η^0	4.0	0.5	0.0	-0.48	-1.0
γ	1.025	0.992	0.667	0.589	0.599
μ_s^0/ε_F^0	0.035	0.358	0.820	1.335	1.544
$R_\perp(\mu$m)	4.12	13.53	20.71	26.12	28.09

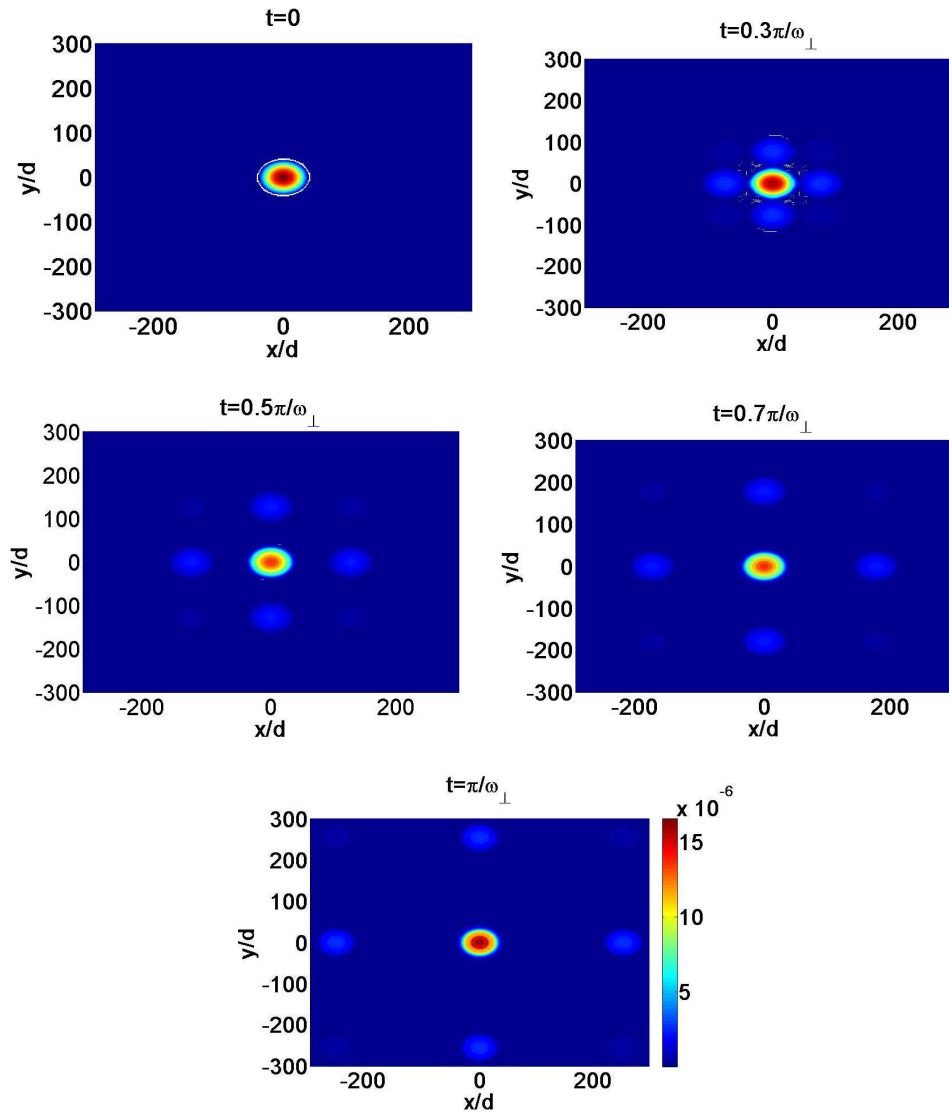

Fig. 1. (Color online) Time evolution of the interference patterns of the superfluid Fermi in the regime of BCS–BEC crossover for $(\eta^0, \gamma, \mu_s^0/\varepsilon_F^0) = (0.5, 0.992, 0.358)$ (i.e., the case (b) of Table 1) when both the parabolic trap and the optical lattice are switched off. Sequent panels in the figure are for time $t = 0$, $t = 0.3\pi/\omega_\perp$, $t = 0.5\pi/\omega_\perp$, $t = 0.7\pi/\omega_\perp$, and $1.0\pi/\omega_\perp$, respectively.

see that interference patterns are not stationary. Although the position of the principal maximum (i.e., the central peak) is not movable, the position of secondary maximums (i.e., the secondary peaks) are not fixed and they are movable as time goes on. In fact, many other high-order secondary maximums exist in the interference patterns, which are not obvious in the figure because of their smaller values

in density. It is easy to obtain the position of the four secondary maximums

$$\mathbf{r}_{\pm 1}(t) = \pm \left[\frac{2\pi\hbar t}{Md}\mathbf{e}_x + \frac{2\pi\hbar t}{Md}\mathbf{e}_y \right], \tag{20}$$

where $\mathbf{e}_x$ and $\mathbf{e}_y$ are unit vectors along x- and y-directions, respectively. Thus the separation between the secondary maximums is proportional to time t. These evolution characters of the interference patterns of the superfluid Fermi gas are due to the quantum property of the system. This point can be easily understood by Eq. (19), in which the parameter α that results in dispersion (and hence expansion) of the condensate wavefunction is proportional to the Planck constant $\hbar$. In addition, Eq. (20) manifests also the quantum property of the interference patterns, since $\hbar$ is also involved.

In order to show different features of the interference patterns in different superfluid regimes of the BCS–BEC crossover, in Fig. 2 we have presented the simulating result of the interference patterns for dimensionless density $n_s(x, y, t)/n_1$ ($n_1 \equiv N/a_{\rm op}$) when the system is released from both the parabolic trap and the optical lattice at $t = 0.4\pi/\omega_\perp$. Interference patterns in panels (a), (b), (c), (d), and (e) are obtained by calculating n_s/n_1 based on the parameters given in the cases (a), (b), (c), (d) and (e) of Table 1. We see that from the BEC regime [case (a)], through the crossover regime [cases (b), (c) and (d)], to the BCS regime [case (e)], the interference peaks become wider and their maxima are also lowered gradually. Plotted in the panel (f) is maximum value of principal interference peak [i.e., $n_s(x = y = 0, t = 0.4\pi/\omega_\perp)/n_1$] as a function of η^0. The physical reason for the change of the interference patterns from the BEC regime to the BCS regime can be explained as follows. Because in the BEC (BCS) regime the reference chemical potential μ_s^0 is smaller (larger), the radius of the condensate $R_\perp$ is smaller (larger) (see Table 1 for detail), which results in a larger (smaller) peak value and narrower (wider) width of the interference peaks in the BEC (BCS) regime. We stress that although such feature exists also in the case of 3D optical lattice, but for the 2D optical lattice considered here the decrease of the value of interference peak from the BEC regime to BCS regime is faster and more obvious, which is advantageous and convenient in experiment for distinguishing different superfluid regimes in the BCS–BEC crossover.

2.3. *Interference patterns after switching off only the optical lattice*

Taking the advantage of the propagator method, we further explore the time evolution of interference patterns of the superfluid Fermi gas in an alternative way. Instead of switching off both the parabolic trap and optical lattice as studied in the last subsection, we now consider the situation of turning off the optical lattice but maintaining the parabolic trap. In this situation the subcondensates evolve inside the parabolic trap for a variable time.

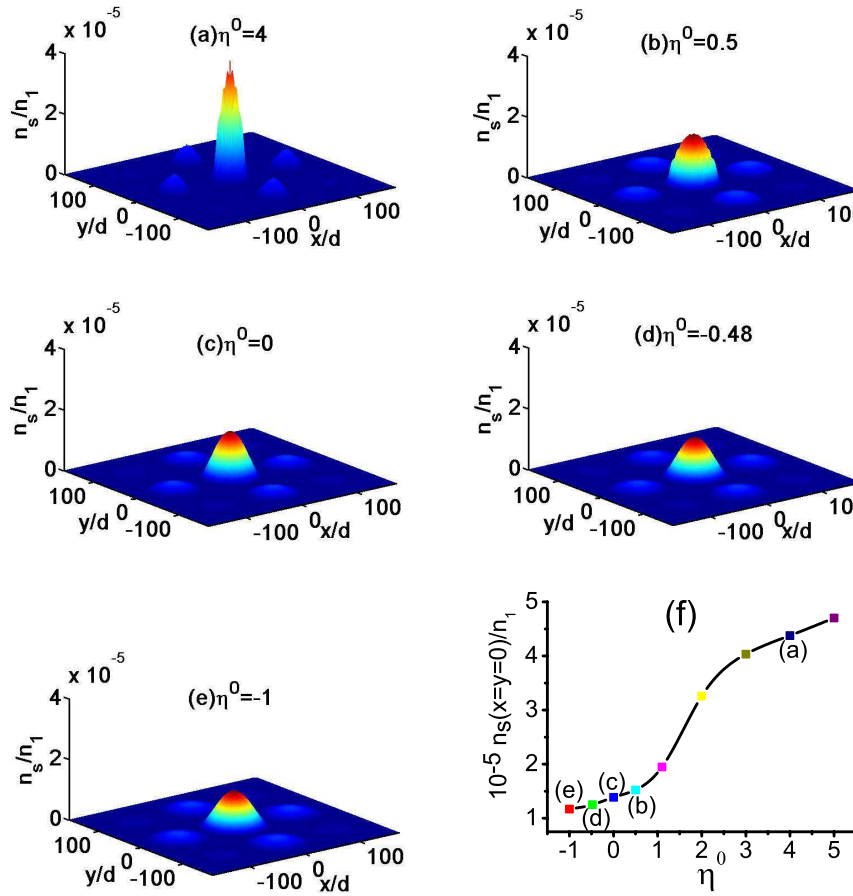

Fig. 2. (Color online) Dimensionless column pair density $n_s(x, y)/n_1$ in the BCS–BEC crossover for time $t = 0.4\pi/\omega_\perp$ when the system is released from both the parabolic trap and the optical lattice. Interference patterns in panels (a)–(e) are obtained based on the parameters given in the cases (a)–(e) of Table 1. Shown in the panel (f) is maximum of principal interference peak [i.e., $n_s(x = y = 0, t = 0.4\pi/\omega_\perp)/n_1$] as a function of η^0.

When only the parabolic trap is kept, the evolution of condensate wavefunction is given by the integration

$$\Psi_s(x, y, t) = \int_{-\infty}^{\infty} dx' \int_{-\infty}^{\infty} dy' K(x, y, t; x', y', t' = 0)\Psi_s(x', y', t' = 0)\,, \tag{21}$$

involved the initial wavefunction of the condensate in the combined trapping, $\Psi(x', y', t' = 0)$, given by Eq. (16), and the propagator for the particles in the parabolic trap

$$K(x, y, t; x', y', t' = 0) = \prod_{j=1}^{2} K_j(x_j, t; x'_j, t' = 0)\,, \tag{22}$$

where

$$K_j(x_j,t;x_j',t'=0)=\left[\frac{M\omega_\perp}{2\pi i\hbar\sin\omega_\perp t}\right]^{1/2}\times\exp\left\{\frac{iM\omega_\perp}{2\hbar\sin\omega_\perp t}\left[(x_j^2+x_j'^{\,2})\cos\omega_\perp t-2x_jx_j'\right]\right\}. \quad (23)$$

with $(x_1,x_2)\equiv(x,y)$.

It is easy to get the following analytical result of $\Psi_s(x,y,t)$ for the evolution of the condensate

$$\Psi_s(x,y,t)=A_n{\sum_{k_x,k_y}}'\left(1-\frac{k_x^2+k_y^2}{k_M^2}\right)^{\frac{2+\gamma}{4\gamma}}\prod_{j=1}^{2}\Xi_j(x_j,t)\,, \quad (24)$$

where

$$\Xi_j(x_j,t)=\left[\frac{1}{\sin\omega_\perp t(\cot\omega_\perp t+i\beta)}\right]^{1/2}\exp\left[-\frac{(x_j-k_jd\cos\omega_\perp t)^2}{2a_{\rm op}^2\sin^2\omega_\perp t(\beta^2+\cot^2\omega_\perp t)}\right]\times\exp\left[-i\frac{\cot\omega_\perp t(x_j-k_jd\cos\omega_\perp t)^2}{2\beta a_{\rm op}^2\sin^2\omega_\perp t(\cot^2\omega_\perp t+\beta^2)}\right]\times\exp\left[i\frac{(x_j^2\cos\omega_\perp t+k_j^2d^2\cos\omega_\perp t-2x_jk_jd)}{2\beta a_{\rm op}^2\sin\omega_\perp t}\right], \quad (25)$$

with $\beta=\hbar/(M\omega_\perp a_{\rm op}^2)$.

Based on the above result, in Fig. 3 we have shown the interference pattern for pair density distribution of the superfluid Fermi gas in the BCS regime characterized by the set of parameters $(\eta^0,\gamma,\mu_s^0/\varepsilon_F^0)=(-1.0,1.544,0.599)$ for the case (e) of Table 1. Sequent panels in the figure are for the time t taking at 0, $0.3\pi/\omega_\perp$, $0.45\pi/\omega_\perp$, $0.7\pi/\omega_\perp$, and $1.0\pi/\omega_\perp$, respectively. The system parameters chosen are $\omega_\perp=2\pi\times200$ Hz, $\omega_z=2\pi\times20{,}000$ Hz, $N=5\times10^4$, $\lambda=1064$ nm, and $s=5$. We see that initially $(t=0)$ there exists a central peak only. As the time goes on the central peak decays and sidepeaks grow gradually. At $t=0.45\pi/\omega_\perp$ the central peak becomes smallest, and then the pattern recovers to the initial shape at $t=1.0\pi/\omega_\perp$. It is found that when t increases further from $1.0\pi/\omega_\perp$ to $2.0\pi/\omega_\perp$, we obtain the same result shown in the figure. Thus the interference pattern exhibits a *periodic decay and revival*, with the oscillating periodicity $\pi/\omega_\perp$.

It is easy to get the analytical expression of the maximum value of the central peak, which reaches its maximum value at time $t_m=(2m-1)\pi/(2\omega_\perp)$, here m is a positive integer. At time t_m, one has

$$n_s(x=y=0,t_m)=N\left(\frac{3\gamma+2}{2\gamma}\right)\left[\frac{M\omega_\perp}{\pi\hbar a_{\rm op}^2k_M}\right]^2\left[{\sum_{k_x,k_y}}'\left(1-\frac{k_x^2+k_y^2}{k_M^2}\right)^{\frac{2+\gamma}{4\gamma}}\right]^2. \quad (26)$$

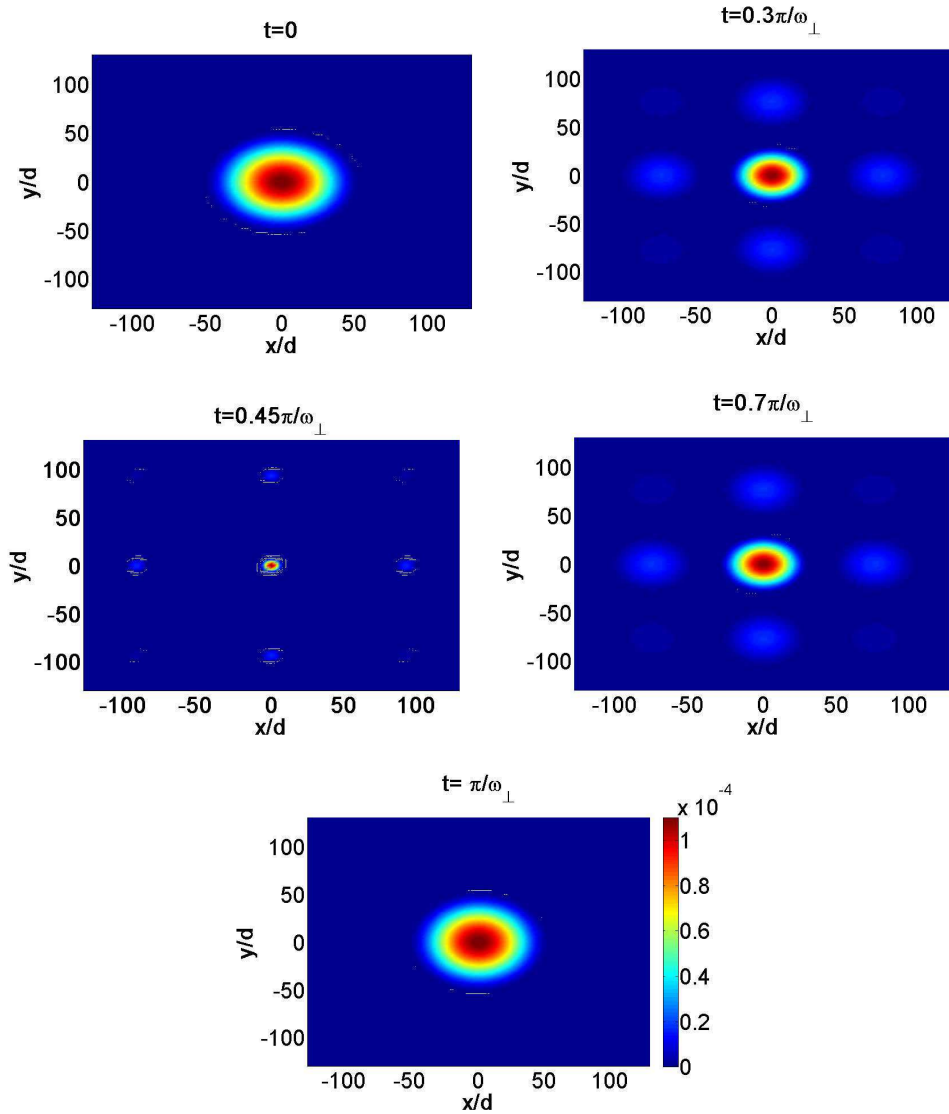

Fig. 3. (Color online) Evolution of the interference pattern of the superfluid Fermi gas when keeping in the parabolic trap but released from the optical lattice. The system parameters are $(\eta^0, \gamma, \mu_s^0/\varepsilon_F^0) = (-1.0, 0.599, 1.544)$. The sequent panels show the patterns for $t = 0$, $0.3\pi/\omega_\perp$, $0.4\pi/\omega_\perp$, and $0.45\pi/\omega_\perp$ respectively.

By transforming the summation for k_x and k_y into an integration, we obtain

$$n_s(x = y = 0, t_m) = 8N\gamma \frac{(3\gamma + 2)}{(2 + 5\gamma)^2} \left(\frac{M\omega_\perp k_M}{\hbar a_{\rm op}^2} \right)^2 . \tag{27}$$

The position of the secondary peaks near the central peak can be obtained

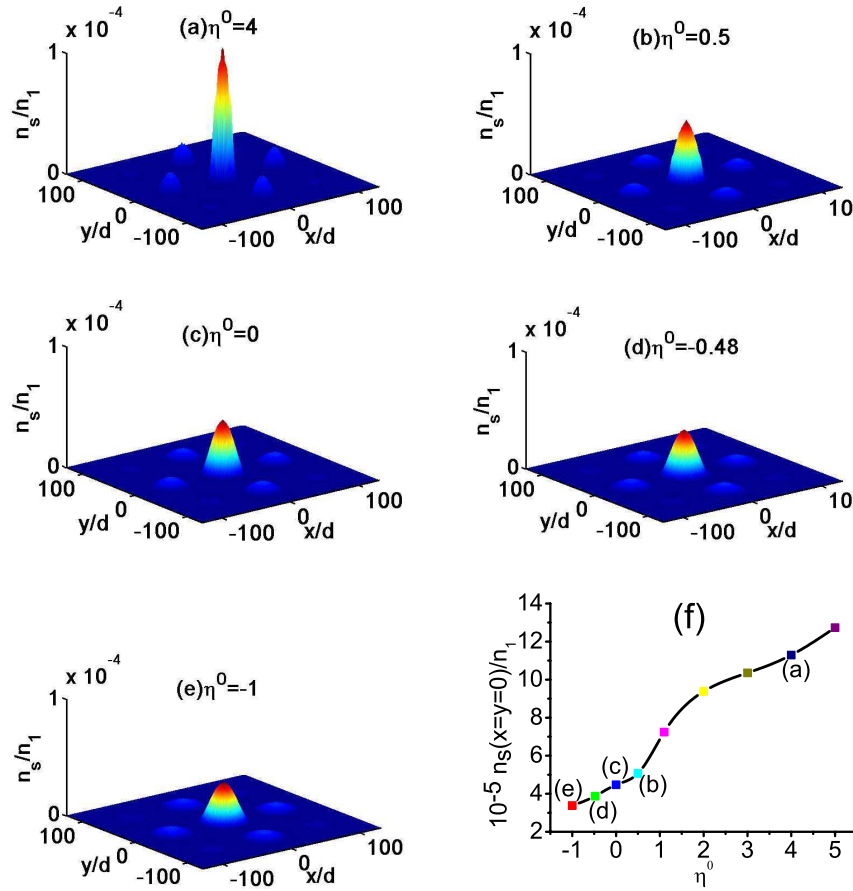

Fig. 4. (Color online) Column pair density distribution $n_s(x, y)$ in the BCS–BEC crossover when the subcondensates have been released from the optical lattice potential for $t = 0.3\pi/\omega_\perp$. The interference in panels (a)–(e) are obtained by calculating $n_s(x, y)$ based on the parameters given in cases (a)–(e) of Table 1. The panel (f) is the maxima of central peak $n_s(x = y = 0)$ as a function of η^0. In all figures the values of pairs density $n_s(x, y)$ have been normalized by $n_1 = N/a_{\rm op}^2$.

analytically, which read

$$\mathbf{r}_{\pm 1}(t) = \pm \left[\frac{2\pi\hbar}{M\omega_\perp d} \sin(\omega_\perp t)\mathbf{e}_x + \frac{2\pi\hbar}{M\omega_\perp d} \sin(\omega_\perp t)\mathbf{e}_y \right]. \tag{28}$$

There are two physical reasons for the oscillating behavior (decay and revival) of the interference pattern. One is due to the confinement of the parabolic trap. The other one arises from the quantum property of the system, which can be seen from the expression of Eq. (25) where the parameter β that contributes dispersion is proportional to the Planck constant $\hbar$.

In order to make a comparison between the interference patterns in different superfluid regimes of the BCS–BEC crossover when only the optical lattice is switched

off, in Fig. 4 we have plotted the simulating result of n_s/n_1 for $t = 0.3\pi/\omega_\perp$. Panels (a), (b), (c), (d), and (e) are obtained for the parameters given in the cases (a), (b), (c), (d) and (e) of Table 1. One can see that from the BEC regime [case (a)], through the crossover regime [cases (b), (c) and (d)], to the BCS regime [case (e)], the interference peaks become wider and their maxima are also lowered gradually. The panel (f) is the maximum value of central peak $n_s(x = y = 0)$ as a function of η^0. Different features of the interference patterns for different superfluid regimes are clearly shown, with the physical reasons being basically the same as that explained in the last subsection.

In the calculation of interference patterns given above, interatomic interaction between atoms has been neglected. Here we make an estimation on the role played by atomic interaction during the expansion of the fermionic atomic gas. The kinetic, potential, and interaction energies of the system are respectively given by

$$E_{\rm kin}(t) = N\int_{-\infty}^{\infty} dx \int_{-\infty}^{\infty} dy \int_{-\infty}^{\infty} dz \frac{\hbar^2}{2M} |\nabla \Psi_s(\mathbf{r}, t)|^2 \,, \tag{29a}$$

$$E_{\rm pot}(t) = N\int_{-\infty}^{\infty} dx \int_{-\infty}^{\infty} dy \int_{-\infty}^{\infty} dz [V_s^{\rm ho}(\mathbf{r}) + V_s^{\rm op}(x, y)] |\Psi_s(\mathbf{r}, t)|^2 \,, \tag{29b}$$

$$E_{\rm int}(t) = N\int_{-\infty}^{\infty} dx \int_{-\infty}^{\infty} dy \int_{-\infty}^{\infty} dz \frac{\mu_s(n_s)}{\gamma + 1} |\Psi_s(\mathbf{r}, t)|^2 \,. \tag{29c}$$

We first estimate above energies before the expansion (i.e., $t = 0$) by considering $\eta^0 = 4$ (i.e., the case (a) of Table 1; BEC regime) and $\eta^0 = -1$ (i.e., the case (e) of Table 1; BCS regime). For $\eta^0 = 4$, we obtain $E_{\rm kin}(0) = 0.72 \times 10^{-18}$ J, $E_{\rm pot}(0) = 0.22 \times 10^{-15}$ J, $E_{\rm int}(0) = 0.43 \times 10^{-13}$ J; For $\eta^0 = -1$, we obtain $E_{\rm kin}(0) = 0.93 \times 10^{-14}$ J, $E_{\rm pot}(0) = 0.32 \times 10^{-11}$ J, $E_{\rm int}(0) = 0.16 \times 10^{-11}$ J. This result tells us that in the ground state (i.e., before the expansion) the interaction energy is very significant and must be taken into account. However, when atoms is released from the optical lattice, the gas expands rapidly, the interatomic interaction decreases rapidly also. This point can be seen by calculating the interaction energy during the expansion. By using above expressions we obtain the ratio of interaction energy to the total energy, i.e., $E_{\rm int}(t)/E(t)$, where the total energy is given by $E(t) = E_{\rm kin}(t) + E_{\rm pot}(t) + E_{\rm int}(t)$. Shown in Fig. 5 is our calculating result. We see that when the atomic gas expands for only 10 microseconds, $E_{\rm int}(t)/E(t)$ decreases to 5% for both cases (i.e. $\eta^0 = 4$ and $\eta^0 = -1.0$). Thus the interaction energy is indeed small during the expansion for a larger time, which is the situation of measurement of interference patterns in experiment.

3. Discussion and Summary

The results given above is obtained based on the GGP equation (1). Although up to now many research works for studying the physical property of superfluid Fermi gases are based on the GGP equation (Refs. 11–25; see also section 3'2.3 of Ref. 2),

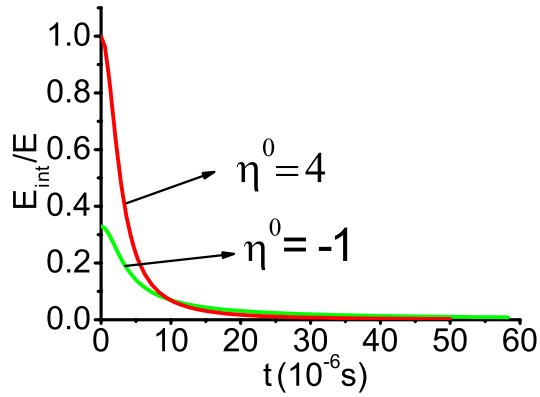

Fig. 5. (Color online) The ratio of interaction energy to the total energy $E_{\rm int}/E$ as a function of time t, for the case $\eta^0 = 4$ and the case $\eta^0 = -1$ during the expansion of the fermionic atomic gas.

no discussion on the limitation of this equation has been provided in literature. In fact, the GGP equation is valid under the following conditions: (i) The system is in a superfluid state, and works at zero temperature or very low temperature with thermal particle playing no significant role. (ii) Particle numbers in two internal (spin) states are equal, and all particle are paired and condensed, i.e., depletion of the condensate play no significant role. (iii) When an external, time-dependent perturbation is applied to the condensate, only low-energy collective excitations are generated, with the excitation energy less than the energy gap of single-particle excitations, i.e., single-particle excitation due to the breaking of Cooper pairs does not occur. (iv) The particle number of the system is large.

In the deep BCS regime (i.e., $\eta^0 \ll -1$) one must be careful when using the GGP equation. The reason is that, for the present-day superfluid Fermi gases realized experimentally, the energy gap $\Delta_{\rm gap}$ of single-particle excitations is small. This can be seen by the formula $\Delta_{\rm gap} = 1.76 k_B T_c$, where T_c is critical temperature. Taking $T_c \approx 200$ nK, we obtain $\Delta_{\rm gap}/h \approx 100\ {\rm s}^{-1}$. Thus a collective excitation with oscillating frequency the same as that of trapping potential (usually between several tens and several hundred Hertz) will break Cooper pairs, i.e., single-particle excitations are unavoidable when collective oscillations are excited in the deep BCS regime with oscillating frequency having the same order as that of the trapping potential. Furthermore, there is another reason for the invalidity of the GGP equation in the deep BCS regime. In fact, in the deep BCS regime and when $\Delta_{\rm gap}$ is small, a quantum depletion of the condensate may be significant. In this case, the GGP equation becomes invalid because it does not include the quantum depletion of the condensate. Of course, if experimental conditions can be improved to increase $\Delta_{\rm gap}$ (which can be realized, e.g., by increasing condensed particle number, hopefully in cold Fermi-gas experiments in future), the GGP equation may be used even in the deep BCS regime. Another way is to add some correction terms in the GGP

equation (1) to include the effects of the pair-breaking and the quantum depletion. Then one will obtain a new, dissipative GGP equation. This is an interesting topic deserving to explore, but beyond the scope of our present work.

In summary, we have made a detailed investigation on the interference patterns and their time evolution of a superfluid Fermi gas in the BCS–BEC crossover. Based on a superfluid order-parameter equation, we have calculated the initial distribution of subcondensates formed in a combined potential of a parabolic trap and a 2D optical lattice. By using the Feynman propagator method combined with numerical simulations we have discussed the interference patterns of the subcondensates for two different cases. The first one is when both the parabolic trap and optical lattice are switched off simultaneously. In this case, interference pattern displays a main peak and secondary peaks. The separation between the interference peaks is proportional to time. The other one is when the 2D optical lattice is switched off but the parabolic trap is maintained. The interference pattern in this case is found to display decay and revival. The decay and revival repeats periodically with increasing time. Such behavior of the interference patterns is due to the quantum property of the superfluid Fermi gas and due to the contribution of the combined potentials that act on the system. We have demonstrated that in the case of 2D optical lattice the interference patterns in different superfluid regimes of the BCS–BEC crossover have more obvious features than that in the case of a 3D optical lattice. Thus it is more convenient to use the 2D optical lattice system to experimentally distinguishing different superfluid regimes of the BCS–BEC crossover. We note that in a recent experiment Martiyanov *et al.*[36] have successfully realized a degenerate fermionic (^{6}Li) atomic gas in 2D, in which the interaction of atoms in the gas can be widely tuned by means of Feshbach resonance. Such system can be used to study the interference patterns predicted in the present work when the system is prepared in an optical lattice.

Acknowledgments

This work was supported by NSF-China under Grant Nos. 10874043, 11174080, and 11105039, and by the Key Development Program for Basic Research of China under Grant Nos. 2005CB724508 and 2006CB921104.

References

1. S. Giorgini, L. P. Pitaevskii and S. Stringari, *Rev. Mod. Phys.* **80**, 1215 (2008), and references therein.
2. W. Ketterle and M. W. Zwierlein, *Riv. Nuovo Cim.* **31**, 247 (2008), and references therein.
3. C. J. Pethick and H. Smith, *Bose–Einstein Condensation in Dilute Gases*, 2nd edn. (Cambridge University Press, Cambridge, 2008), Chap. 17.
4. I. Bloch, *Science* **319**, 1202 (2008).
5. O. Morsch and M. Oberthaler, *Rev. Mod. Phys.* **78**, 179 (2006), and references therein.
6. G. Roati *et al.*, *Nature* **453**, 895 (2008).

7. U. Schneider *et al.*, *Science* **322**, 1520 (2008).
8. L. Hackermüller *et al.*, *Science* **327**, 1621 (2010).
9. W. Wen, Y. Zhou and G. Huang, *Phys. Rev. A* **77**, 033623 (2008).
10. J. K. Chin *et al.*, *Nature* **443**, 961 (2006).
11. Y. E. Kim and A. L. Zubarev, *Phys. Rev. A* **70**, 033612 (2004).
12. J. Catani *et al.*, *Phys. Rev. A* **77**, 011603(R) (2005).
13. N. Manini and L. Salasnich, *Phys. Rev. A* **71**, 033625 (2005).
14. T. K. Ghosh and K. Machida, *Phys. Rev. A* **73**, 013613 (2006).
15. G. Diana, N. Manini and L. Salasnich, *Phys. Rev. A* **73**, 065601 (2006).
16. J. Yin, Y. L. Ma and G. Huang, *Phys. Rev. A* **74**, 013609 (2006).
17. L. Salasnich and N. Manini, *Laser Phys.* **17**, 169 (2007).
18. Y. Zhou and G. Huang, *Phys. Rev. A* **75**, 023611 (2007).
19. W. Wen and G. Huang, *Phys. Lett. A* **362**, 331 (2007).
20. Y.-L. Ma and G. Huang, *Phys. Rev. A* **75**, 063629 (2007).
21. L. Salasnich, N. Manini and F. Toigo, *Phys. Rev. A* **77**, 043609 (2008).
22. A. L. Zubarev, *J. Phys. B* **42**, 011001 (2009).
23. A. L. Zubarev, *Europhys. Lett.* **87**, 33001 (2009).
24. W. Wen and G. Huang, *Phys. Rev. A* **79**, 023605 (2009).
25. W. Wen, S. Shen and G. Huang, *Phys. Rev. B* **81**, 014528 (2010).
26. G. E. Astrakharchik *et al.*, *Phys. Rev. Lett.* **93**, 200404 (2004).
27. J. Carlson *et al.*, *Phys. Rev. Lett.* **91**, 050401 (2003)
28. S.-Y. Chang *et al.*, *Phys. Rev. A* **70**, 043602 (2004).
29. P. Pieri and G. C. Strinati, *Phys. Rev. Lett.* **91**, 030401 (2003).
30. C. Menotti, P. Pedri and S. Stringari, *Phys. Rev. Lett.* **89**, 250402 (2002).
31. H. Heiselberg, *Phys. Rev. Lett.* **93**, 040402 (2004).
32. H. Hu *et al.*, *Phys. Rev. Lett.* **93**, 190403 (2004).
33. P. Pedri *et al.*, *Phys. Rev. Lett.* **87**, 220401 (2001).
34. S. Liu *et al.*, *J. Phys. B* **36**, 2083 (2003).
35. R. P. Feynman and A. R. Hibbs, *Quantum Mechanics and Path Integrals* (McGraw-Hill, New Work, 1965).
36. K. Martiyanov, V. Makhalov and A. Turlapov, *Phys. Rev. Lett.* **105**, 030404 (2010).